

SpRET: Highly Sensitive and Reliable Spectral Measurement of Absolute FRET Efficiency

Shiri Levy, Christian D. Wilms, Eliaz Brumer, Joy Kahn, Lilach Pnueli, Yoav Arava, Jens Eilers and Daniel Gitler

SUPPLEMENTARY INFORMATION

1. Calibration of SpRET

Precise calibration is paramount to achieve instrument-independent measurements of absolute E values, and is in essence what sets SpRET apart from other FRET measurement methodologies. To perform SpRET, several categories of calibration parameters are measured. These include: spectral-sensitivity calibration curves, spectral fingerprints of the participating fluorescent moieties, the acceptor scaling factor (SF), and the acceptor-to-donor molar-ratio normalization factor (P_{AD}).

1.1 Spectral-sensitivity calibration

The basis for quantitative determination of E by SpRET is the ability to derive values that are linearly proportional to the number of emitted photons out of fluorescence measurements that are inherently instrument-specific. Although the detector array of the Nikon C1Si is precalibrated and linearized, this calibration may not take into account all relevant optical components such as the objective, and especially the primary dichroic mirror. Therefore, we produced spectral-sensitivity calibration curves (Supplementary Figure S1 A,C) that reflect the instrument response to a NIST (National Institute of Standards and Technology) precalibrated reference light source (LS-1-CAL, Ocean Optics, Dunedin FL). The lamp's light was fed into the oil-immersion objective through a drop of Nikon immersion oil placed on a #1 coverslip, or into the water-dipping objective through saline placed on a coverslip (the coverslips themselves did

not affect the correction curves, data not shown). Distinct curves were produced for each combination of optical components (objective, dichroic mirror, detector array, specimen tray etc). The calibration curves were multiplied by the nominal wavelength to transform them from energy units to values related to photon counts (Supplementary Figure S1 B,D). The resultant curves are stable over time but should be produced periodically, in case of changes in the spectral properties of the optical system or the detectors.

1.2 Spectral fingerprints of fluorescent components

Knowledge of the emission spectra of the fluorescent components of the sample is needed in order to quantitatively separate the total emissions into fluorophore-specific contributions by linear unmixing (Zimmermann, et al., 2003). In our system, spectral fingerprints of four components were necessary to produce satisfactory fits: donor, acceptor, cellular autofluorescence and background (Table 1, main document, Supplementary Figure S2). When spectral aberrations were not negligible, two different donor spectral fingerprints were needed (see below).

To obtain an average background spectrum, 8 to 10 images depicting cells transfected with a control pcDNA3 plasmid were acquired. In each image, spectra were obtained from several (typical 2-5) regions of interest (ROIs) devoid of cells. The spectra were normalized area-wise, and a mean spectrum was calculated. This procedure was repeated for both excitation wavelengths, producing the spectral

fingerprints BG_S^{405} and BG_S^{488} (Supplementary Figure S2 A).

Spectral fingerprints of cellular autofluorescence (AU_S^{405} and AU_S^{488} , Supplementary Figure S2 B) were characterized in the same manner, but from ROIs placed over cells in the aforementioned images. Because the acquired spectra were contaminated to various degrees by the spectral fingerprint of the background, a novel refinement procedure (see below) was used to extract the pure autofluorescence spectra. We stress that AU_S^{405} and AU_S^{488} are not necessarily similar in form due to differential excitation of unknown autofluorescent molecules by the two excitation wavelengths. Note that autofluorescence spectra differ between cell-types.

The spectral fingerprint of the donor (D_S) and the acceptor (A_S) were characterized from cells expressing either the donor or the acceptor, using the 405 and 488 nm excitation lines, respectively (Supplementary Figure S2 C-D). When possible, spectra were acquired from cells exhibiting fluorescence intensities significantly greater than those typical for autofluorescence or background, to minimize the contribution of the latter. Notwithstanding, the degree of contamination of donor or acceptor spectra by autofluorescence or by background was typically not negligible. Therefore, refinement (see below) was developed to produce pure spectra (Supplementary Figure S2 C-E).

1.3 Refinement of spectral fingerprints

Our novel refinement procedure is based on the assumption that the individual acquired spectra that are used to derive spectral fingerprints are composed of linear combinations of ad-hoc unknown pure spectral fingerprints of the background, autofluorescence, and of the donor or acceptor (as applicable) at undetermined proportions, i.e., the

individual acquired spectra are contaminated to varying degrees by other components. However, it follows that for each separate contaminant, there exists a sampled instance that is minimally contaminated. This instance may not be directly usable as a spectral fingerprint due to its noise content, or alternatively, it may be additionally contaminated by a different contaminant.

The spectral fingerprint of the background is deemed pure by definition. Refinement of the autofluorescence spectral fingerprint involves removal of background contamination. Refinement of the donor or acceptor involves removal of both background and autofluorescence, assuming the autofluorescence spectrum was refined first. In the interest of simplicity, the refinement procedure is explained in Supplementary Figure S3 as applying to the donor spectral fingerprint (and is applied in the same manner to autofluorescence and acceptor spectra). The robustness of the refinement procedure is illustrated by the similarity of spectra refined from dim cells, where the raw spectra are substantially contaminated, and from strongly expressing cells (Supplementary Figure S2 E), where the relative contribution of the contaminations in the raw data is much lesser.

2. Subtraction of direct excitation (DE) fraction

An additional factor that limits accurate determination of FRET is direct excitation (DE) of the acceptor because DE may be interpreted as a false-positive FRET signal. Careful choice of the excitation lasers can limit DE , but typically does not eliminate it; nevertheless, DE is assessed using a scaling factor (SF , Figure 1, main document) based on images obtained when exciting exclusively the acceptor. The significance of subtracting DE is

exemplified by the similarity of the emission spectrum obtained from cells exhibiting weak FRET (expressing Cer20Ven and excess cerulean) and from cells expressing cerulean and an excess of venus, in which FRET does not occur (Supplementary Figure S4 and see Figure 6 A-B in main document). Although both spectra are indistinguishable, the acceptor component of the former is due to *SE* and in the latter it is due to *DE*.

3. Chromatic aberrations and their correction

In some microscopy applications the use of objectives that are not fully corrected for chromatic aberrations (like many water-dipping objectives) is unavoidable. Under such conditions, the spectral response of the system depends on the focal plane, degrading the quality of fitting and the precision of *E*. We found that the spectral fingerprint of cyan fluorescent protein changed along the focal axis (Supplementary Figure S5 A), without affecting the acceptor's spectral fingerprint. Importantly, all measured donor emissions, notwithstanding the focal plane, could be represented as linear combinations of donor spectra obtained from planes farthest (D1) and closest (D2) to the substratum (Supplementary Figure S5 A-B). Using both D1 and D2 concurrently, as spectral fingerprints of the donor, significantly improved fitting of spectra from cells expressing Cer20Ven. Furthermore, a linear relationship was evident between *E* and the relative fraction of D1 out of donor emissions (Supplementary Figure S5 C), where:

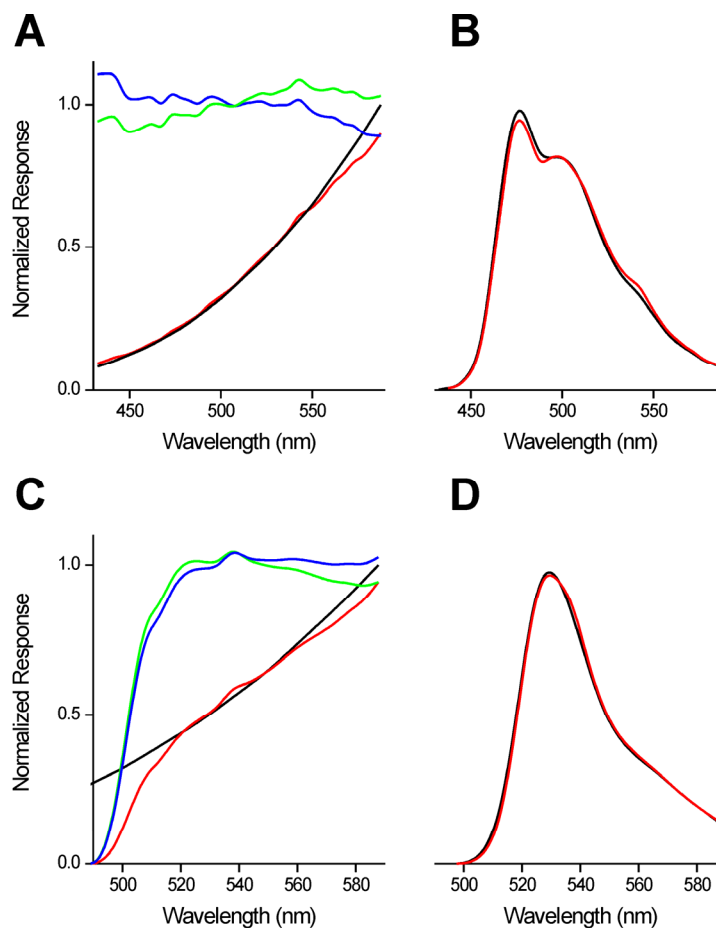
$$D1\% = 100 \times W_{D1}^{405} / (W_{D1}^{405} + W_{D2}^{405}).$$

This relationship illustrates a systematic deviation of up to 10% in the calculated *E* values that is related to the chromatic aberration. To correct for this deviation, the slope and intercept of the linear regression was determined (Supplementary Figure S5 C) and an objective-specific correction parameter $NS = \text{slope}/\text{intercept}$ was calculated (*NS* is specific to the acquisition settings). *E* values were corrected by multiplication by $(1 - NS \times D1\%)$. The same approach was used to correct the effect of chromatic aberrations on the acceptor-to-donor molar ratio, for which a similar but inverse linear relationship was observed. Importantly, this procedure was not necessary when using fully-corrected objectives, such as the CFI Plan Apochromat VC 60X oil immersion 1.4NA objective (Nikon, Japan). To characterize the chromatic aberration inherent to the imaging conditions and to calculate the correction parameter *NS* (if it is indeed necessary), Z-stacks of samples expressing exclusively the donor should be produced and analyzed as described to define D1 and D2, followed by determination of the linear relationship between *E* and D1% in Z-stacks of samples exhibiting FRET (the specific *E* value is not of consequence).

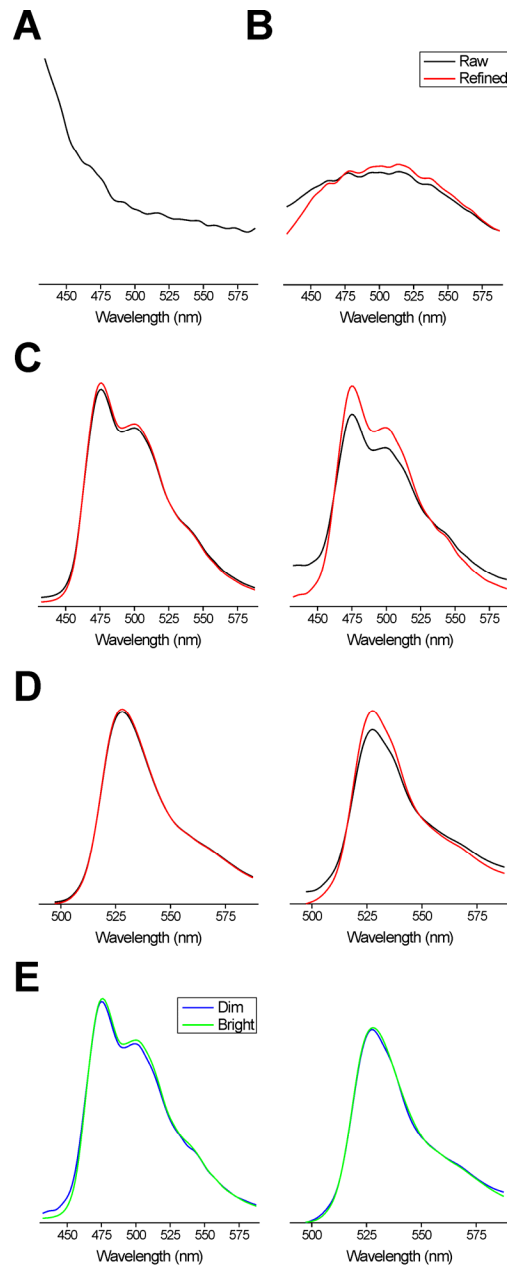
REFERENCES

- ZIMMERMANN, T., RIETDORF, J. & PEPPERKOK, R. (2003). Spectral imaging and its applications in live cell microscopy. *FEBS Lett.* **546**(1), 87-92.

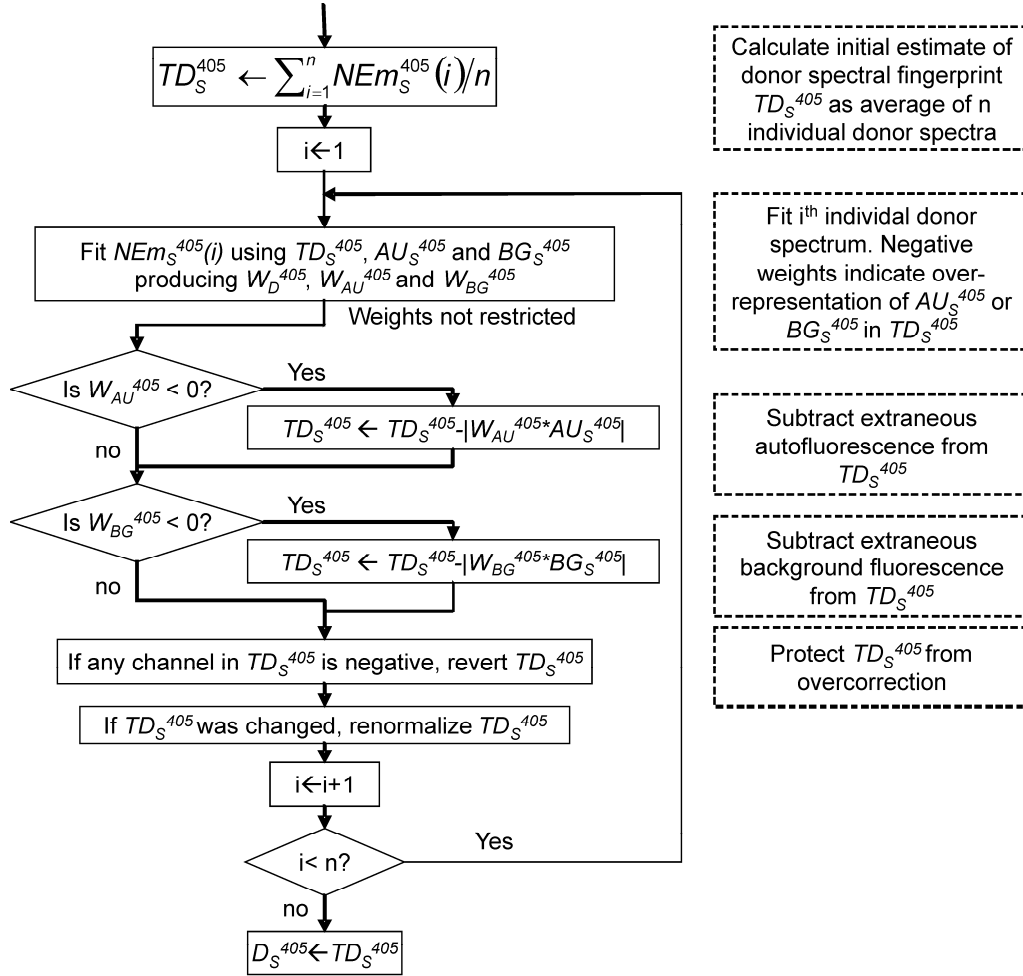
SUPPLEMENTARY FIGURES



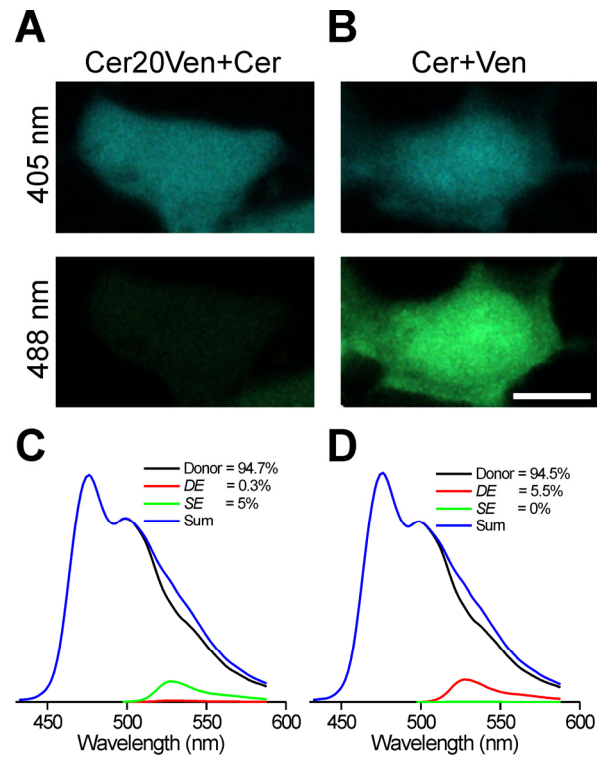
Supplementary figure S1: Spectral correction of acquired spectra. (A) Black line: reference spectrum of NIST calibrated lamp in the range of 430-590 nm. Red line: spectrum of NIST lamp measured with our confocal microscope using the 405 nm primary dichroic mirror and the 60X NA 1.0 water dipping objective. Blue line: ratio between measured and reference spectra. Green line: same after multiplication by nominal wavelength value and renormalized at 500nm. (B) Black line: cerulean spectral fingerprint before correction of spectral sensitivity. Red line: same, after correction using green curve in (A). (C) same as (A) except spectra were measured using the 488 nm dichroic mirror in the range of 495-590 nm. (D) Same as (B), except for venus spectral fingerprint.



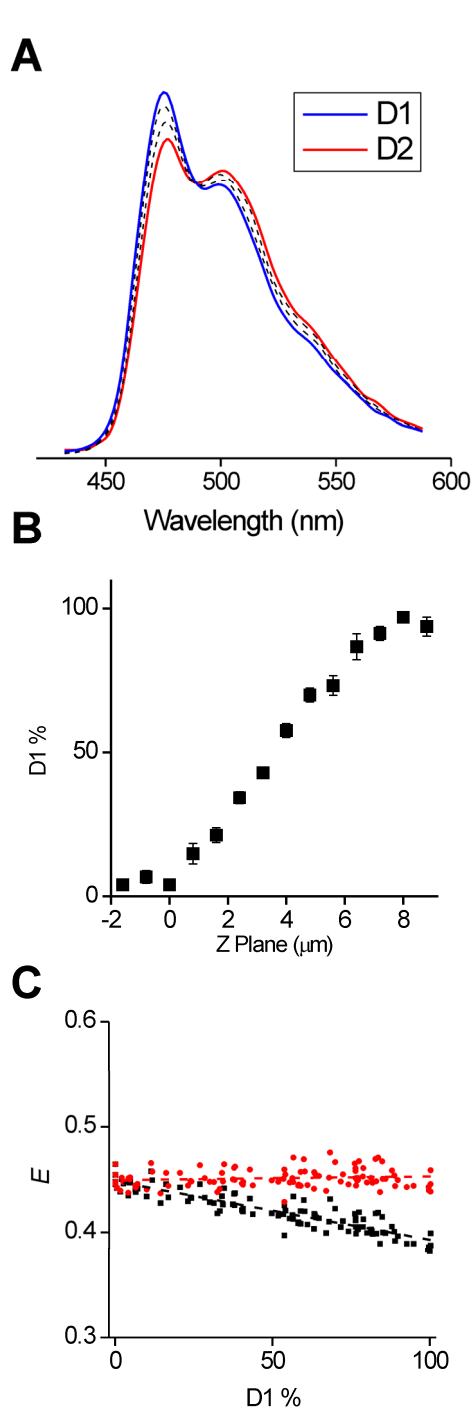
Supplementary figure S2: Spectral fingerprints and their refinement. (A) Spectral fingerprint of background. (B) Unrefined (black line) and refined (red line) spectral fingerprints of autofluorescence of HEK cells. (C) like (B) but for cerulean fluorescence. (D) like (B) but for venus fluorescence. In (C) and (D), left traces are of raw and refined spectral fingerprints obtained from brightly expressing cells and right traces are from dimly expressing cells, where contamination by background and autofluorescence is significant. (E) Overlay of refined spectral fingerprints obtained from dim (blue) and bright (green) cells. Note that the refined spectral fingerprints obtained under both conditions are similar.



Supplementary figure S3: Flowchart for refining spectral fingerprints. For clarity purposes, refinement of the donor spectral fingerprint is explained. An initial estimate of the spectral fingerprint of the donor (TD_S^{405}) is produced by averaging n area-normalized emission spectra ($NEm_S^{405}(1..n)$) obtained from cells expressing exclusively the donor. Assuming that each of $NEm_S^{405}(1..n)$ contains donor, autofluorescence and background, then TD_S^{405} is a linear combination of these three components. TD_S^{405} is refined by serially ($i=1..n$) fitting $NEm_S^{405}(i)$ using TD_S^{405} and the previously acquired pure spectral fingerprints BG_S^{405} and AU_S^{405} , allowing the weights W_{BG}^{405} and W_{AU}^{405} to be negative. A negative weight indicates that $NEm_S^{405}(i)$ contains less background or autofluorescence than TD_S^{405} ; if this is the case, $|W_{BG}^{405} * BG_S^{405}|$ or $|W_{AU}^{405} * AU_S^{405}|$ are subtracted from TD_S^{405} , in order to attain in TD_S^{405} the lesser level of contamination found in $NEm_S^{405}(i)$. If altered, TD_S^{405} is renormalized before progressing to the next member in the series $NEm_S^{405}(i)$. To avoid overcorrection, if any of the 32 channels of TD_S^{405} is negative after the described adjustment, TD_S^{405} is reverted to its value one step backwards. D_S^{405} , the final refined spectral fingerprint of the donor, is set to be TD_S^{405} after processing all n instances of $Em_S^{405}(i)$ in this manner.



Supplementary figure S4: Comparison of *SE* to *DE*. (A) Live HEK cell expressing Cer20Ven and excess cerulean, exhibiting overall weak FRET. Emissions due to excitation with 405 nm (top) and 488 nm (bottom) laser lines. Scale bar: 10 μ m. (B) Like (A), but cell expressing unlinked cerulean and venus, which do not express FRET. (C) donor (black), *SE* (red) and *DE* (green) components of 405 nm induced emissions and sum for cell shown in (A). (D) Like (C), except for cell shown in (B). Although the sum of emissions in (C) and (D) are indistinguishable, acceptor emission in (C) is due to *SE* and in (D) due to *DE*.



Supplementary figure S5: Correction of the deviation of E due to chromatic aberrations. (A) Area-normalized cerulean emission spectra obtained from the top (D1, blue) and bottom (D2, red) of spectral z-stacks (14 planes, $0.8 \mu\text{m}$ apart) of cerulean-expressing HEK cells. Emission spectra from two representative intermediate planes are shown as dashed black lines. (B) Spectra obtained from within the z-stack are linear combinations of D1 and D2. Depicted is the percentage of D1 contribution to the total emission of cerulean (D1%) as a function of the distance from the face of the coverslip. (C) E was calculated at various z-planes taken from HEK cells ($n=6$) expressing Cer20Ven. Fitting was performed using D1 and D2 as two spectral fingerprints for the donor. Total donor contribution was calculated as the sum of the weights of D1 and D2. E was plotted as a function of D1% (black squares). Chromatic aberration causes a linear deviation of E from the value observed on the face of the coverslip (black dashed line). The same data are shown after correcting for the deviation as described in the text (red squares and dashed line).